ACS APPLIED MATERIALS & INTERFACES

Research Article

www.acsami.org

Janus Si Micropillar Arrays with Thermal-Responsive Anisotropic Wettability for Manipulation of Microfluid Motions

Tieqiang Wang,[†,‡] Hongxu Chen,[†] Kun Liu,[†] Shuli Wang,[†] Peihong Xue,[†] Ye Yu,[†] Peng Ge,[†] Junhu Zhang,*[,†] and Bai Yang[†]

[†]State Key Laboratory of Supramolecular Structure and Materials, College of Chemistry, Jilin University, Changchun, 130012, P. R. China

[‡]Research Center for Molecular Science and Engineering, College of Science, Northeastern University, Shenyang 110004, P. R. China

Supporting Information

ABSTRACT: In this paper, Janus micropillar array (MPA) with fore−aft controllable wettability difference was demonstrated. With two-step modification process, we successfully decorate the Janus pillar skeletons with wettability-switchable polymer brush on one side and hydrophilic self-assembled monolayer on the other. Owing to the switchable wettability of the polymer brush, the patterned surface could switch between anisotropic wetting and isotropic wetting at different temperatures, which gives the possibility of coupling the well-designed surface with microfluidic channel to manipulate the microfluid motion. Additionally, a further photothermal control of microfluid was also established based on the thermal-responsive Janus MPA through introducing infrared light to adjust the temperature of the microfluidic system. We believe that the thermal-responsive Janus micropillar arrays would provide a new strategy to control the flow and motion of fluids in microfluidic channels and show potential applications in the future microfluidic chips.

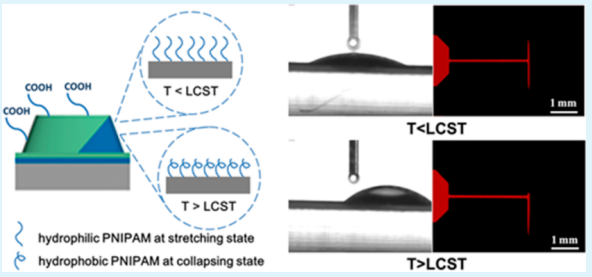

KEYWORDS: *thermoresponsive, Janus pillar array, anisotropic wetting, smart microfluidic manipulation*

INTRODUCTION

Asymmetric microstructures inspired from Mother Nature have great importance due to their unique physical properties, such as anisotropic wetting, anisotropic adhesion, and directional transmission, and they have received extensive attention for a wide range of applications in microfluidic devices, dry adhesives, and three-dimensional displays.[1−13] More specifically, asymmetric microstructures with anisotropic wettability, owing to their liquid motion handling ability, have been reviewed in detail several times,[1−3] and a number of asymmetric microstructures with anisotropic wettability have been successfully fabricated using conventional lithography techniques and unconventional techniques involving molding, embossing, etching, and surface wrinkling.[14−21] Moreover, some research has been done to guide liquid flow in a single direction, and such achievements have been expected to control liquid flow in microfluidic assays, in which sequential delivery of multiple reagents in detection regions and temporally controlled reagent transport are strongly needed.[22]

Recently, Yoon et al. have successfully realized the in situ fabrication of asymmetric microstructures in microfluidic channels by photopolymerization of liquid prepolymers in a channel according to the selective light refraction into one direction through the optical Lucius prism array, and such work offers great possibility for the application of asymmetric microstructures in microfluidic system.[23] Additionally, considering the future smart microfluidic system, it would be more interesting if asymmetric microstructures with tunable anisotropic wettability were introduced within microchannels to manipulate fluid motion in response to various external stimuli.[2] However, to the best of our knowledge, no works have been reported utilizing asymmetric microstructures with responsive anisotropic wetting properties to intelligently manipulate fluid motion. Suh et al. have reported a responsive unidirectional wetting behavior on a two-face prism array;[24] however, owing to the strip structure and the relatively large period of the prism, it is difficult to integrate such surface into microfluidic system. Thus, fabrication of other novel microstructures with responsive anisotropic wetting properties and integration of such microstructures within microchannels is still urgently expected to construct smart microfluidic systems and intelligently manipulate fluid motion.

Previously, we reported the strategy of oblique deposition and selective modification for the fabrication of Janus Si micropillar arrays (Si-MPAs). Owing to the opposite wettability of the molecule modified on opposite sides of the Janus Si pillars, the Janus arrays showed peculiar anisotropic surface wetting behavior and were then used to prepare one-way valve

Received: September 16, 2014
Accepted: December 5, 2014
Published: December 5, 2014

of microfluidic system based on their outstanding anisotropic wettability.[25,26] Recently, responsive polymer brushes fabricated by surface-initiated atom-transfer radical polymerization (SI-ATRP) have attracted immense interest due to their potential in responsive surfaces.[27−37] Therefore, combining responsive polymer brushes with such anisotropic wetting microstructures may be a hopeful strategy to fabricate reversible switching anisotropic wetting surfaces and to further intelligently manipulate fluid motion in microfluidic channels. Herein, thermal-responsive poly(*N*-isopropylacrylamide) (PNIPAM) brushes are introduced to the Janus Si pillar arrays for the fabrication of thermal-responsive surface. When the PNIPAM molecule switches between hydrophilic and hydrophobic at temperature below or above the lower critical solution temperature (LCST) of PNIPAM molecule, the thermal-responsive surface could switch between isotropic wetting and anisotropic wetting. The responsive surface shows excellent reversibility and quick switching speed through comparing with other similar thermal-responsive brush systems.[35−37] Moreover, through coupling with microfluidic channel, the thermal-responsive Janus arrays show great abilities to manipulate the liquid flowing direction in the microfluidic system by altering the temperature. Finally, a further proof-of-concept photo-thermal microfluid-control process was also established through tuning the temperature of the fluidic system under the irradiation with infrared lamp.

EXPERIMENTAL SECTION

Materials. Silicon substrates were cleaned by immersion in piranha solution (3:1 concentrated H_2SO_4/30% H_2O_2) for 1 h at 70 °C to create a hydrophilic surface and then rinsed repeatedly with Milli-Q water (18.2 MΩ cm) and ethanol. The substrates were dried in nitrogen gas before use. Polydimethylsiloxane (PDMS) elastomer kits (Sylgard 184) were purchased from Dow Corning (Midland, MI). Copper(I) chloride (CuCl), aminopropyl trimethoxysilane (ATMS), bromoisobutyryl bromide, *N*-isopropylacrylamide (NIPAM), and 16-mercaptohexadecanoic acid (MHA) were all purchased from Aldrich. Pentamethyl diethylene triamine (PMDETA) was perchased from TCI (Shanghai). Sulfuric acid, hydrogen peroxide, triethylamine, and methanol were used as received. The glass microfluidic chip was obtained from Key Lab of Analytical Chemistry for Life Science Nanjing University.

Preparation. The elliptical Si micropillar arrays were prepared through an etching method using a PS elliptical hemisphere arrays as the etching mask, which was reported in our previous work.[25] To fabricate Janus Si-MPAs, a layer of PNIPAM (~20 nm) was first polymerized onto the surface of the elliptical pillars through SI-ATRP.[32] Then, through oblique deposition, a thin film of gold was deposited onto one side of the polymer-brush-coated micropillars. Finally, selective modification of MHA onto Au surface was performed through immersing the Janus array into an ethanol solution of MHA with concentration of ~4 mM. To fabricate T-shaped microfluidic channel, the PDMS microfluidic channel was peeled from the microfluidic chip, then connected with an automatic sample injector, and finally compressed onto the surface of the Janus Si pillar arrays.

Characterization. Scanning electron microscopy (SEM) micrographs were taken with a JEOL FESEM 6700F electron microscope with primary electron energy of 3 kV. A heating stage was placed under the sample to control the temperature of the whole system; to avoid the temperature fluctuation of the whole system, a temperature (60 °C) much higher than LCST of PNIPAM was used to realize the switching of wettability. The chemical compositions were determined by X-ray photoelectron spectroscopy (XPS, Thermo ESCALAB 250) in the area of ~500 × 500 μm^2. The wetting behavior of 20 μL water droplet on the surface of Janus array was recorded using a drop shape analysis system (DSA 10 MK2, KRÜSS) at saturated humidity. The flowing behavior of Rhodamine B aqueous solution in the microfluidic channel was recorded with an Olympus fluorescence microscope (BX51).

RESULTS AND DISCUSSION

3.1. Fabrication of the Janus MPAs with Thermal-Responsive Surface Modification. The procedure for the fabrication of thermal-responsive Janus MPAs is shown in Figure 1. As reported before,[26] if the morphology of the Si-MPA skeleton is elliptical, the anisotropic wettability of the Janus MPAs can be enhanced. Therefore, Si-MPAs with elliptical morphology were first fabricated via etching method as reported before.[25] The SEM image of the elliptical Si-MPA Figure 2a clearly shows the asymmetric morphology of the

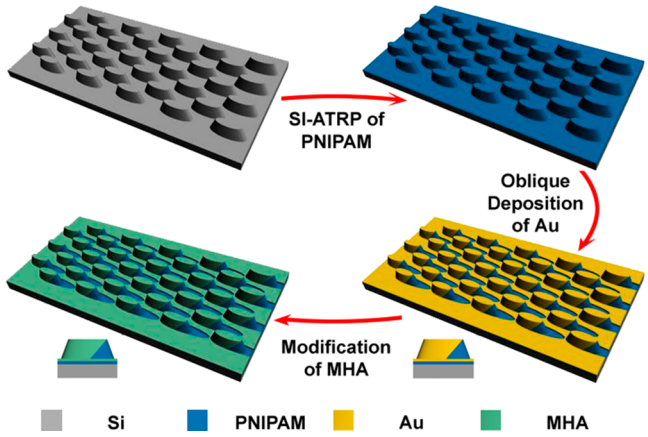

Figure 1. A schematic illustration of the procedure for the fabrication of PNIPAM/MHA Janus Si pillar arrays.

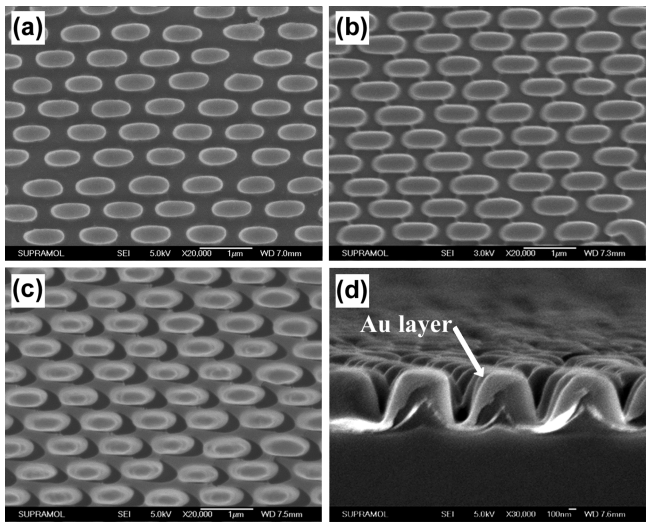

Figure 2. SEM images of the as-prepared Si-EPA framework (a) before and (b) after the SI-ATRP of PNIPAM and (c) the Janus Si-EPA. (d) The cross-section SEM image of the Janus Si-EPA.

micropillars (long axis: ~1050 nm; short axis: ~340 nm). After the fabrication of elliptical Si-MPA skeleton, the surface of the Si-MPAs was modified with a thin layer (~20 nm) of PNIPAM brush by SI-ATRP. Figure 2b shows the SEM image of the Si-MPA after the SI-ATRP of PNIPAM; it clearly shows that the surface of the Si-MPAs is smoother after the modification of PNIPAM due to the coating of a thin polymer layer, and there

dx.doi.org/10.1021/am5063647 | ACS Appl. Mater. Interfaces 2015, 7, 376−382

are many threadlike connections between the adjacent elliptical pillars. As we all know, the PNIPAM molecule is a famous thermal-responsive molecule, whose LCST is ~32 °C;[32] thus, owing to the thermal responsiveness of PNIPAM molecule, the surface of the PNIPAM-coated Si-MPAs is hydrophobic at a temperature above the LCST of PNIPAM and hydrophilic at a temperature below that (Supporting Information, Figure S1). Next, to make the Si pillars Janus-constructed, oblique Au deposition process was performed. The SEM image and the cross-section SEM image of the Janus Si-EPA are shown in Figure 2c,d. The dark crescent-shaped shadows aside the elliptical silica pillars indicate that a full fore−aft morphology is generated successfully, which could also be drawn from the cross-section view. After the deposition of Au layer, a self-assembled monolayer of hydrophilic 16-mercaptohexadecanoic acid (MHA) molecule was selectively modified on the surface of the gold based on the covalent bond between gold and thiol group of MHA molecule. Finally, one side of the Si pillars was covered with thermal-responsive PNIPAM brushes, and the other side was covered with hydrophilic MHA self-assembled monolayer, which means that the Si pillars were Janus-modified and that the surface wettability of one side of the Si pillars was thermal-responsive.

To prove the Janus structure of the Si pillar arrays, XPS measurement of the Si-MPAs during the fabrication process was also employed as shown in Figure 3a. Through comparing the XPS survey spectrum of the Si-EPA (black line) with the PNIPAM-modified ones (red line), the N_{1s} peak at 398 eV found in the XPS spectrum of the PNIPAM-modified Si-MPAs means that the PNIPAM molecule was successfully bonded onto the Si surface through SI-ATRP. After the oblique deposition of gold, both N_{1s} peak at 398 eV (Figure 3b) and Au_{4f} peak at 86 eV exist in the XPS survey spectrum of the Janus arrays, which indicates that during the oblique deposition of gold, only part of the PNIPAM modified Si pillar array is deposited with gold, while another part of the Si pillar array is still modified by thermal-responsive PNIPAM molecules. As a comparative sample, if Au was vertically deposited onto the surface of the PNIPAM-coated MPA, all the surface of the MPA would be coated by Au layer according to the disappeared N_{1s} peak (Supporting Information, Figure S2). After the oblique deposition of gold, MHA monolayer was modified on the surface of Au, the S_{2p} peak (Figure 3c) proves the successful modification of MHA molecule. In addition, as shown in the XPS spectrum (pink line of Figure 3a), the intensity of Au_{4f} peak is weakened, while the intensity of N_{1s} peak (Figure 3d) maintained, which, to some extent, indicates that the hydrophilic MHA molecule was selectively attached to the top of the gold, while the PNIPAM-modified area was still unchanged. The XPS measurements show the Janus nature of the pillars, and two sides of the Janus Si pillars were covered with hydrophilic MHA layer and thermal-responsive PNIPAM layer, respectively.

3.2. Thermal-Responsive Wetting Behavior of the Janus Si Pillar Arrays. Since one side of the Janus pillars is modified with thermal-responsive PNIPAM brushes, the surface wettability of the Janus pillars will change at different temperature as illustrated in Figure 4a. When the system temperature is below the LCST of PNIPAM, both sides of the Janus Si-EPA are hydrophilic; thus, the surface exhibits isotropic wettability, and the water drop spreads along both the PNIPAM-modified directions and the MHA-modified direction (Figure 4b). When the temperature of the system is

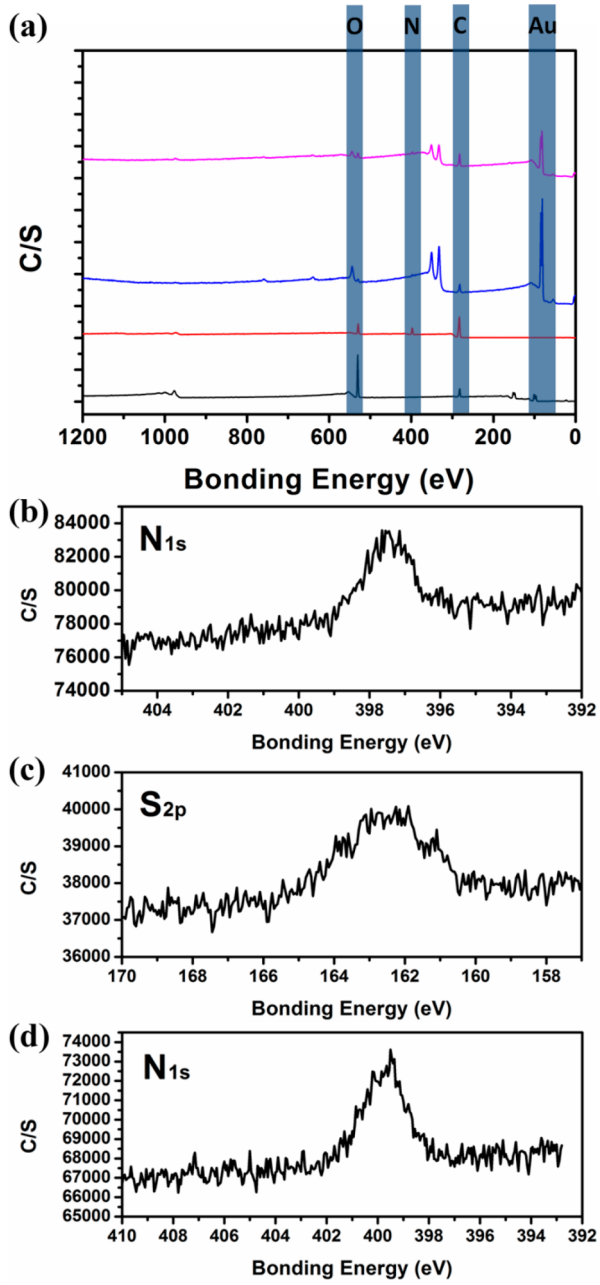

Figure 3. (a) The X-ray photoelectron spectroscopy of the Si-EPA (black), PNIPAM-modified Si-MPAs (red), and the Janus Si-MPAs before (blue) and after (pink) the MHA modification. (b, d) The N_{1s} survey of the Janus Si-MPAs before and after the MHA modification, respectively. (c) The S_{2p} survey of the Janus Si-MPAs after the MHA modification.

above the LCST of PNIPAM, the PNIPAM-modified side of the Janus array switches from hydrophilic to hydrophobic, while the MHA-modified side remains hydrophilic. Because of the unique Janus structure of the Si-MPAs, when the gas−liquid−solid triphase contact line is moving across the Janus pillars on the surface, it is easier for the contact line to be pinned on the hydrophilic uphill side of the Janus pillars than the contact line to be pinned on the hydrophobic uphill side. Therefore, if the two sides of the Janus pillar are modified by hydrophilic (MHA) and hydrophobic (PNIPAM) molecule, respectively, the as-prepared surface exhibits peculiar anisotropic wetting property, and the water drop only wets along the hydrophilic

dx.doi.org/10.1021/am5063647 | ACS Appl. Mater. Interfaces 2015, 7, 376−382

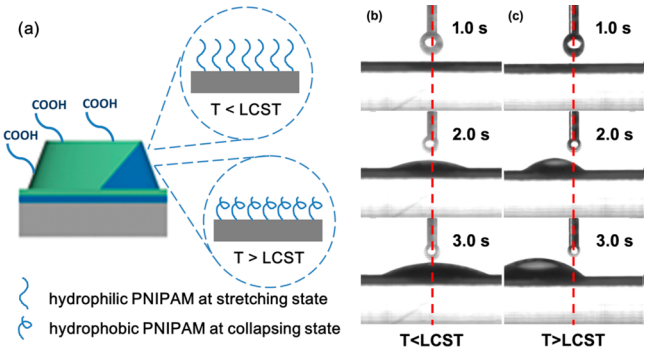

Figure 4. (a) A schematic illustration of the PNIPAM/MHA Janus pillar surface wettability at different temperatures. (b, c) The photographs of the water drop taken at different time after the water drop contacted the surface of PNIPAM/MHA Janus array at a temperature below and above the LCST of PNIPAM brush. The red dotted line is the center axis of the syringe needle.

MHA-modified direction, while the three-phase contact line at the hydrophobic PNIPAM-modified side is pinned on the surface (Figure 4c). This indicates that when the temperature is below or above the LCST of PNIPAM, the wetting property of the Janus Si-MPAs is switchable between isotropic wetting and anisotropic wetting due to the switching of PNIPAM brushes between hydrophilic and hydrophobic. Additionally, the advancing angle of the thermal-responsive MPA was also measured at different direction to support the thermal-responsive anisotropic wettability. When the temperature is below the LCST of PNIPAM, the advancing angle in both directions is almost equal (59.5° in the MHA-modified direction and 59.8° in the PNIPAM-modified direction); however, when the system temperature increases to that above the LCST of PNIPAM, the advancing angle in different direction becomes anisotropic (67.2° in the MHA-modified direction and 85.1° in the PNIPAM-modified direction). These results well support the anisotropic wettability of the thermal-responsive Janus MPA.

As a surface with switchable wettability, reversibility is one crucial important parameter for its further application performance; thus, the responsive reversibility of the Janus Si-MPAs was also investigated, which is shown in Figure 5. According to the photographs of a 20 μL waterdrop on the Janus Si-MPA (inset of Figure 5), the wetting distance along the PNIPAM-modified direction and that along the MHA-modified direction is defined as D_{PNIPAM} and D_{MHA}, respectively, and the ratio between these two quantities (D_{PNIPAM}/D_{MHA}) is used to evaluate the surface wetting property of the thermal-responsive Janus Si-MPA ("1" represents the ideal isotropic wetting surface, while "0" represents the ideal anisotropic wetting behavior). These results show excellent reversibility for more than 100 cycles and a quick conversion between isotropic wettability and anisotropic wettability (the switch duration is less than 1 min) through comparing with other similar thermal-responsive brush systems.[35−37] Additionally, to prove the reversibility of the thermoswitchable surface, the repeatability of the average surface energy was also explored through measuring the contact angle as shown in Supporting Information, Figure S3. This reversibility still remained after the samples had been laid aside for at least one week. We believe that the excellent reversibility results from the stability of the Si-EPA framework and the strong covalent interaction between the Si-EPA framework and the surface modification molecules.

3.3. Smart Microfluid Manipulation Based on the Responsive Janus Si-MPAs. Since the PNIPAM/MHA Janus Si-MPAs showed excellent thermal responsiveness between isotropic wetting and anisotropic wetting, we believe that the as-prepared Janus Si-MPAs will show smart abilities to manipulate the liquid motion in microfluidic channels. To investigate the microfluid manipulation ability of the Janus Si-MPAs, a T-shaped PDMS microfluid channel was coupled with the Janus Si-MPAs, and the flowing behavior of water in the microfluidic channel was studied. The schematic of the microfluidic channel was illustrated in Figure 6a, the Janus Si-MPAs were positioned at the T-junction of channel, and the MHA-modified direction of the Janus MPA was orientated along one outlet direction of the T-shaped microfluidic channel for the unidirectional flow of the microfluid, which is perpendicular to the injected direction of microfluid. The microscope photograph and the detail size parameters of the T-shaped microfluidic channel are given in Supporting Information, Table S1, and to facilitate the observation of the fluid motion, fluorescent Rhodamine aqueous solution was used. Figure 6b,c shows the fluorescence microscope photographs of the Rhodamine aqueous solution injected into the T-shaped microfluidic channel under different temperature. As

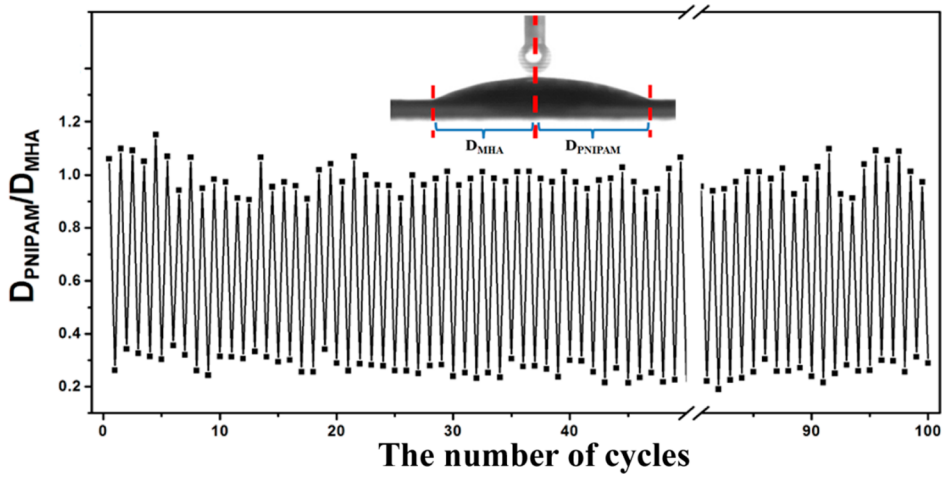

Figure 5. Reproducibility of the thermal-responsive Janus pillar arrays. Half cycles: 20 °C; and integral cycles: 60 °C.

dx.doi.org/10.1021/am5063647 | ACS Appl. Mater. Interfaces 2015, 7, 376−382

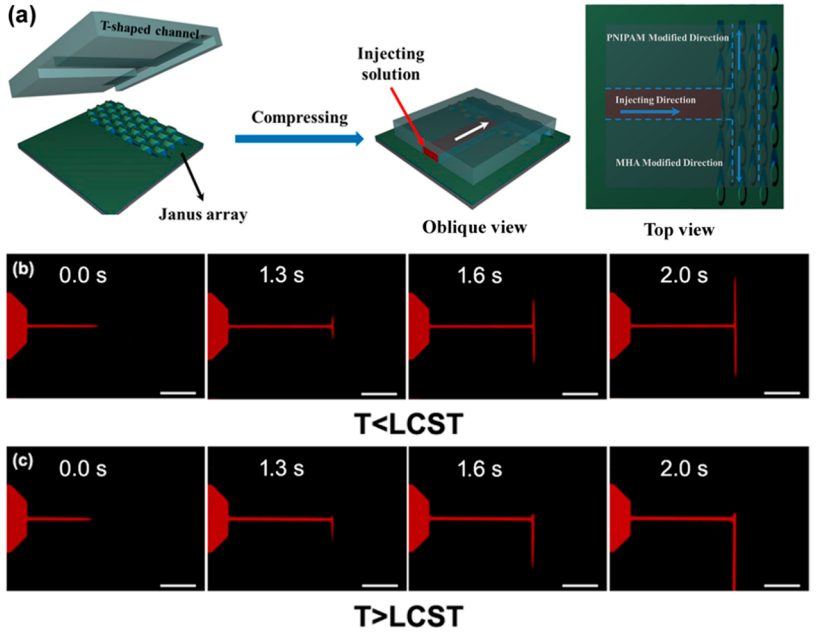

Figure 6. (a) The schematic fabricating process of the T-shaped microfluidic channel. (b, c) The fluorescence microscope photographs of the Rhodamine aqueous solution injected into a T-shaped microfluidic channel taken at different time when the temperature is below and above the LCST of PNIPAM. The scale bars are 1000 μm, and the downward direction is the MHA-modified direction.

shown in Figure 6b, when the system temperature was below the LCST of PNIPAM, due to the isotropic wettability of the Janus arrays under this condition, the aqueous solution flowed freely along both directions of the channel without any differences, meaning that both of the channels were open under temperature below the LCST of PNIPAM. When the system temperature was increased above the LCST of PNIPAM, the surface wettability of the Janus array would switch from isotropic wettability to anisotropic wettability, and water would only wet along the hydrophilic MHA modified direction. Thus, the aqueous solution only flowed into the channel toward the MHA-modified direction, while there was little aqueous solution passing the channel in the PNIPAM-modified direction (Figure 6c). Since the interaction between hydrophobic PDMS channel wall and the aqueous solution is negligible, it could be indicated from the different microfluid flow behavior that the as-prepared responsive Si-MPAs could smartly manipulate the microfluid according to the system temperature even without any other external control unit.

Next, on the basis of switchable flowing behaviors of the aqueous solution, a waterflow behavioral control was performed by tuning the temperature from 60 to 20 °C and back to 60 °C for the second time as shown in Figure 7a. When the system temperature was above the LCST of PNIPAM molecule (~60 °C), the Janus arrays result in the unidirectional flow of the aqueous solution. After the system temperature was decreased below the LCST of PNIPAM molecule (~20 °C), the channel in the PNIPAM-modified direction "opened", and the Rhodamine solution flowed into both of channels. To close the channel in the PNIPAM-modified direction, the system temperature was increased to ~60 °C for the second time. Under this condition, the unidirectional flow of the solution was recovered, and the channel in the PNIPAM-modified direction was "closed" again. The close−open−close procedure means that the as-prepared thermal-responsive Janus Si-MPAs can serve as a proof-of-concept thermovalve in the microfluidic channel, while the transition speed is relatively slow compared

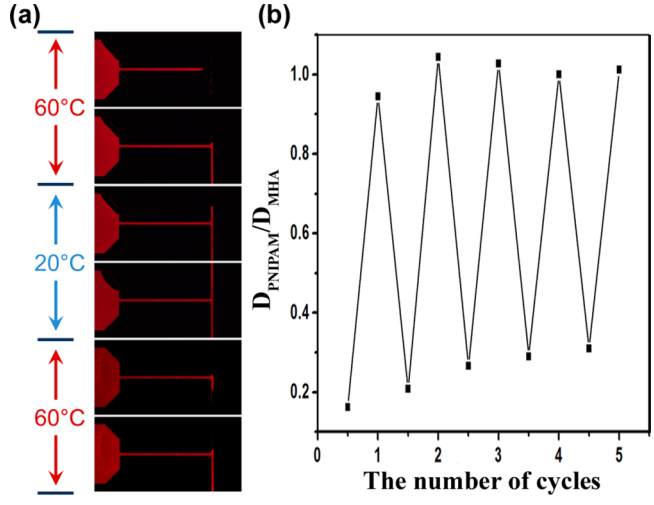

Figure 7. (a) A close−open−close procedure of the microchannel through varying the temperature of the ambient temperature. The downward direction is the MHA-modified direction. (b) The reproducibility of the thermal-responsive microvalve in microfluidic channel. Half cycles: 60 °C; and integral cycles: 20 °C.

with surface wettability changes (the switch time is over 5 min). Additionally, thanks to the excellent reversibility of the PNIPAM/MHA Janus Si-MPAs, the as-prepared thermovalve could also be open and closed several times just by altering the system temperature (Figure 7b). However, in our system, the manipulation of microfluid could only be achieved under low liquid pressure, which means that the fluid flux passing the thermovalve is limited. Therefore, to realize the practical application of such thermovalve, the pressure resistance of the valve must be improved, and we believed that structure optimization and appropriate selection of the surface-modified molecule would be helpful to solve the pressure-resistance problem.

dx.doi.org/10.1021/am5063647 | ACS Appl. Mater. Interfaces 2015, 7, 376−382

As we all know, optical and electrical energy can be easily transformed to thermal mode and trigger the temperature variation. To further exhibit the potential microfluidic applications of the thermal-responsive Janus MPAs, a simple photothermal microfluid-control process was also performed through illuminating the system using an infrared lamp (Figure 8). Because of the heat produced by the infrared lamp, the whole system could be heated to a temperature of ~60 °C; thus, the as-prepared Janus array showed anisotropic wettability (Supporting Information, Figure S4), and the aqueous solution only flowed along the MHA-modified direction (Figure 8a–c). After turning off the infrared lamp, the system cooled to room temperature rapidly, and the as-prepared Janus array showed isotropic wetting property; therefore, the microchannel in the PNIPAM-modified direction was opened, and the aqueous solution flowed along both directions (Figure 8d–f). This to some extent means that a photothermal microfluid-control process could also be realized based on the responsive Janus Si-MPAs, which is of great importance toward current integrated microfluidic devices and lab-on-a-chip system.

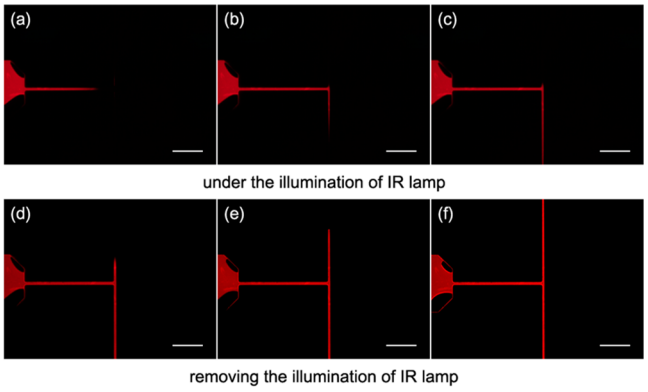

Figure 8. Fluorescence microscope photographs of the Rhodamine aqueous solution injected in a T-shaped microfluid channel (a–c) when the sample and the channel was illuminated using an infrared lamp, and (d–f) after the infrared lamp was turned off. The scale bars are 1 mm. The downward direction is the MHA-modified direction.

CONCLUSIONS

In summary, a thermal-responsive surface based on PNIPAM/MHA Janus Si micropillar array was fabricated by combining SI-ATRP, oblique evaporation, and selective modification. The as-prepared thermal-responsive Janus arrays switched between anisotropic wetting and isotropic wetting when the temperature was above or below the LCST of PNIPAM molecule. Moreover, through coupling a T-shaped PDMS microchannel with the Janus array, we found that the as-prepared thermal-responsive Janus arrays showed great abilities to manipulate the liquid motion in the microfluidic system. This indicates that the thermal-responsive MPA can serve as a proof-of-concept smart thermovalve in microfluidic channel. Additionally, through introducing infrared lamp to adjust the temperature of the microfluidic system, a photothermal microfluid-control process could also be realized based on the responsive Janus Si-MPAs. We believe that the thermal-responsive Janus Si-MPAs would show potential applications in the future microfluidic chips. Additionally, it is also expected to fabricate intelligent microfluidic devices, especially stimuli-responsive valves or switches, based on the Janus Si pillar arrays through modifying the surface of the Janus Si pillar arrays with stimuli-responsive materials.

ASSOCIATED CONTENT

Supporting Information

The contact angle of a 3 μL water drop on the PNIPAM-modified Si pillar array at different temperature; the X-ray photoelectron spectroscopy of the Si-EPA deposited with gold vertically; the contact angles of the PNIPAM/MHA Janus Si pillar arrays at two different temperatures; the wetting behavior of water droplet on the surface of PNIPAM/MHA Janus array under the illumination of the infrared lamp; the microscope photograph, and the detail size parameters of the T-shaped PDMS channel. This material is available free of charge via the Internet at http://pubs.acs.org.

AUTHOR INFORMATION

Corresponding Author

*E-mail: zjh@jlu.edu.cn. Fax: +86-0431-85193423. Phone: +86-0431-85168478.

Notes

The authors declare no competing financial interest.

ACKNOWLEDGMENTS

This work was supported by the National Basic Research Program of China (2012CB933800), the National Natural Science Foundation of China (Grant Nos. 21222406, 21474037, 21404021, 91123031, 21221063), the Program for New Century Excellent Talents in University, Doctoral Fund of Ministry of Education of China (20130061110019), the Fundamental Research Funds for the Central Universities (N130305002), Science and Technology Development Program of Jilin Province, and the Doctoral Scientific Research Foundation of Liaoning Province (20141013). We thank Prof. J. Xu and Dr. B. Xu from Key Lab of Analytical Chemistry for Life Science Nanjing University for the fabrication of the glass MF chip.

REFERENCES

(1) Hancock, M. J.; Sekeroglu, K.; Demirel, M. C. Bioinspired Directional Surfaces for Adhesion, Wetting, and Transport. *Adv. Funct. Mater.* **2012**, *22*, 2223–2234.
(2) Xia, D.; Johnson, L. M.; López, G. P. Anisotropic Wetting Surfaces with One-Dimesional and Directional Structures: Fabrication Approaches, Wetting Properties and Potential Applications. *Adv. Mater.* **2012**, *24*, 1287–1302.
(3) Kwak, M. K.; Jeong, H.-E.; Kim, T.-i.; Yoon, H.; Suh, K. Y. Bio-Inspired Slanted Polymer Nanohairs for Anisotropic Wetting and Directional Dry Adhesion. *Soft Matter* **2010**, *6*, 1849–1857.
(4) Kim, T.-i.; Suh, K. Y. Unidirectional Wetting and Spreading on Stooped Polymer Nanohairs. *Soft Matter* **2009**, *5*, 4131–4135.
(5) Malvadkar, N. A.; Hancock, M. J.; Sekeroglu, K.; Dressick, W. J.; Demirel, M. C. An Engineered Anisotropic Nanofilm with Unidirectional Wetting Properties. *Nat. Mater.* **2010**, *9*, 1023–1028.
(6) Chu, K.-H.; Xiao, R.; Wang, E. N. Uni-Directional Liquid Spreading on Asymmetric Nanostructured Surfaces. *Nat. Mater.* **2010**, *9*, 413–417.
(7) Jokinen, V.; Leinikka, M.; Franssila, S. Microstructured Surfaces for Directional Wetting. *Adv. Mater.* **2009**, *21*, 4835–4838.
(8) Kubus, L.; Erdogan, H.; Piskin, E.; Demirel, G. Controlling Unidirectional Wetting via Surface Chemistry and Morphology. *Soft Matter* **2012**, *8*, 11704–11707.
(9) Jeong, H. E.; Lee, J.-K.; Kim, H. N.; Moon, S. H.; Suh, K. Y. A Nontransferring Dry Adhesive with Hierarchical Polymer Nanohairs. *Proc. Natl. Acad. Sci. U. S. A.* **2009**, *106*, 5639–5644.

(10) Murphy, M. P.; Aksak, B.; Sitti, M. Gecko-Inspired Directional and Controllable Adhesion. *Small* **2009**, *5*, 170−175.
(11) Boesel, L. F.; Greiner, C.; Arzt, E.; del Campo, A. Gecko-Inspired Surfaces: A Path to Strong and Reversible Dry Adhesives. *Adv. Mater.* **2010**, *22*, 2125−2137.
(12) Yoon, H.; Oh, S.-G.; Kang, D. S.; Park, J. M.; Choi, S. J.; Suh, K. Y.; Char, K.; Lee, H. H. Arrays of Lucius Microprisms for Directional Allocation of Light and Autostereoscopic Three-Dimensional Displays. *Nat. Commun.* **2011**, *2*, 455.
(13) Kosako, T.; Kadoya, Y.; Hofmann, H. F. Directional Control of Light by a Nano-Optical Yagi−Uda Antenna. *Nat. Photonics* **2010**, *4*, 312−315.
(14) Xia, D.; Ku, Z.; Lee, S. C.; Brueck, S. R. J. Nanostructures and Functional Materials Fabricated by Interferometric Lithography. *Adv. Mater.* **2011**, *23*, 147−179.
(15) Wu, D.; Chen, Q.; Yao, D. J.; Guan, Y. C.; Wang, J. N.; Niu, L. G.; Fang, H. H.; Sun, H. B. A Simple Strategy to Realize Biomimetic Surfaces with Controlled Anisotropic Wetting. *Appl. Phys. Lett.* **2010**, *96*, 053704.
(16) Liu, L.; Jacobi, A. M.; Chvedov, D. A Surface Embossing Technique to Create Micro-Grooves on an Aluminum Fin Stock for Drainage Enhancement. *J. Micromech. Microeng.* **2009**, *19*, 035026.
(17) Zhang, F.; Low, H. W. Anisotropic Wettability on Imprinted Hierarchical Structures. *Langmuir* **2007**, *23*, 7793−7798.
(18) Chen, F.; Zhang, D.; Yang, Q.; Wang, X.; Dai, B.; Li, X.; Hao, X.; Ding, Y.; Shi, J.; Hou, X. Anisotropic Wetting on Microstrips Surface Fabricated by Femtosecond Laser. *Langmuir* **2011**, *27*, 359−365.
(19) Yang, S.; Khare, K.; Lin, P.-C. Harnessing Surface Wrinkle Patterns in Soft Matter. *Adv. Funct. Mater.* **2010**, *20*, 2550−2564.
(20) Zhang, J. H.; Yang, B. Patterning Colloidal Crystals and Nanostructure Arrays by Soft Lithography. *Adv. Funct. Mater.* **2010**, *20*, 3411−3424.
(21) Zhang, J. H.; Li, Y. F.; Zhang, X. M.; Yang, B. Colloidal Self-Assembly Meets Nanofabrication: From Two-Dimensional Colloidal Crystals to Nanostructure Arrays. *Adv. Mater.* **2010**, *22*, 4249−4269.
(22) Fu, E.; Lutz, B.; Kauffman, P.; Yager, P. Controlled Reagent Transport in Disposable 2D Paper Networks. *Lab Chip* **2010**, *10*, 918−920.
(23) Bae, W. G.; Kimm, S. M.; Choi, S. J.; Oh, S. G.; Yoon, H.; Char, K.; Suh, K. Y. In Situ Realization of Asymmetric Ratchet Structures within Microchannels by Directionally Guided Light Transmission and Their Directional Flow Behavior. *Adv. Mater.* **2014**, *17*, 2665−2670.
(24) Kim, S. K.; Kang, D. H.; Koh, J. H.; Suh, H. S.; Yoon, H.; Suh, K. Y.; Char, K. Thermoresponsive Switching of Liquid Flow Direction on a Two-Face Prism Array. *Soft Matter* **2013**, *9*, 4145−4149.
(25) Wang, T. Q.; Li, X.; Zhang, J. H.; Wang, X. Z.; Zhang, X. M.; Zhang, X.; Zhu, D. F.; Hao, Y. D.; Ren, Z. Y.; Yang, B. Elliptical Silicon Arrays with Anisotropic Optical and Wetting Properties. *Langmuir* **2010**, *26*, 13715−13721.
(26) Wang, T. Q.; Chen, H. X.; Liu, K.; Li, Y.; Xue, P. H.; Yu, Y.; Wang, S. L.; Zhang, J. H.; Kumacheva, E.; Yang, B. Anisotropic Janus Si Nanopillar Arrays as a Microfluidic One-Way Valve for Gas−Liquid Separation. *Nanoscale* **2014**, *6*, 3846−3853.
(27) Barbey, R.; Lavanant, L.; Paripovic, D.; Schüwer, N.; Sugnaux, C.; Tugulu, S.; Klok, H.-A. Polymer Brushes via Surface-Initiated Controlled Radical Polymerization: Synthesis, Characterization, Properties, and Applications. *Chem. Rev.* **2009**, *109*, 5437−5527.
(28) Jain, P.; Baker, G. L.; Bruening, M. L. Applications of Polymer Brushes in Protein Analysis and Purification. *Annu. Rev. Anal. Chem.* **2009**, *2*, 387−408.
(29) Matyjaszewski, K.; Tsarevsky, N. V. Nanostructured Functional Materials Prepared by Atom Transfer Radical Polymerization. *Nat. Chem.* **2009**, *1*, 276−288.
(30) Ma, H. W.; Hyun, J. H.; Stiller, P.; Chilkoti, A. Non-Fouling" Oligo(Ethylene Glycol)-Functionalized Polymer Brushes Synthesized by Surface-Initiated Atom Transfer Radical Polymerization. *Adv. Mater.* **2004**, *16*, 338−341.
(31) Schüwer, N.; Klok, H.-A. A Potassium-Selective Quartz Crystal Microbalance Sensor Based on Crown-Ether Functionalized Polymer Brushes. *Adv. Mater.* **2010**, *22*, 3251−3255.
(32) Sun, T. L.; Wang, G. J.; Feng, L.; Liu, B. Q.; Ma, Y. M.; Jiang, L.; Zhu, D. B. Reversible Switching between Superhydrophilicity and Superhydrophobicity. *Angew. Chem., Int. Ed.* **2004**, *43*, 357−360.
(33) Xia, F.; Feng, L.; Wang, S. T.; Sun, T. L.; Song, W. L.; Jiang, W. H.; Jiang, L. Dual-Responsive Surfaces that Switch between Superhydrophilicity and Superhydrophobicity. *Adv. Mater.* **2006**, *18*, 432−436.
(34) Gao, J.; Liu, Y.; Xu, H.; Wang, Z.; Zhang, X. Biostructure-Like Surfaces with Thermally Responsive Wettability Prepared by Temperature-Induced Phase Separation Micromoding. *Langmuir* **2010**, *26*, 9673−9676.
(35) Chen, Q.; Kooij, E. S.; Sui, X.; Padberg, C. J.; Hempenius, M. A.; Schon, P. M.; Vancso, G. J. Collapse from the Top: Brushes of Poly(N-isopropylacrylamide) in Co-Nonsolvent Mixtures. *Soft Mater.* **2014**, *10*, 3134−3142.
(36) Sui, X.; Chen, Q.; Hempenius, M. A.; Vancso, G. J. Probing the Collapse Dynamics of Poly(N-isopropylacrylamide) Brushes by AFM: Effects of Co-Nonsolvency and Grafting Densities. *Small* **2011**, *7*, 1440−1447.
(37) Koenig, M.; Magerl, D.; Philipp, M.; Eichhorn, K. J.; Muller, M.; Muller-Buschaum, P.; Stamm, M.; Uhlmann, P. Nanocomposite Coatings with Stimuli-Responsive Catalytic Activity. *RSC Adv.* **2014**, *4*, 17579−17586.